# Design of CPW-Fed High Rejection Triple Band-Notch UWB Antenna on Silicon with Diverse Wireless Applications

**Manish Sharma[1], Yogendra K. Awasthi[2, *], and Himanshu Singh[3]**

**Abstract**—In this paper, a CPW-fed circular patch UWB-extended bandwidth antenna is proposed which is fabricated and characterized on silicon. The proposed antenna covers fractional bandwidth of 132.08% with high rejection triple band-notch characteristics [WiMAX(3.30 GHz–3.80 GHz)/WLAN(IEEE802.11a/h/j/n 5.15 GHz–5.35 GHz, 5.25 GHz–5.35 GHz, 5.47 GHz–5.725 GHz, 5.725 GHz–5.825 GHz)/X-band downlink satellite communication system (7.25 GHz–7.75 GHz)]. Gain and efficiency of the proposed antenna in the entire bandwidth vary between 3.96 dBi–10.98 dBi and 84%–95%, respectively. Also, group delay in the entire operating band is $\leq 1.0$ ns. Furthermore, the proposed antenna exhibits good dipole like radiation pattern in $E$-plane and omnidirectional pattern in $H$-plane with small dimension of $20 \times 20 \times 0.5$ mm$^3$.

## 1. INTRODUCTION

Ultra-wideband technology was mainly used for military and radar applications. In recent times, it is widely utilized for ambit of short-range high-throughput wireless communications, medical imaging, ad-hoc networking, high-resolution, reliable data, low power consumption, high immunity to multi-path interferences, high channel capacity and high security measures. Also UWB technology has been developed into most promising technology since Federal Communications Systems (FCC) defined UWB bandwidth (3.10 GHz–10.60 GHz) for various unlicensed applications as this technology offers high performance in the indoor & outdoor wireless communications systems in 2002 [1]. UWB bandwidth is obtained by etching circular ring radiating patch and rectangular ground plane with two small slots near the feed line. WiMAX and WLAN notched bands are obtained by introducing two arc-shaped elliptical slots, and to obtain third notched band for X-band downlink satellite communication system, a pair of single rectangular single split ring resonators is used [2]. By etching arc-shaped slots corresponding to quarter-wavelength or introducing split ring resonators (SRR) near the feed line, a triple-notched UWB antenna is obtained [3]. A lamp-post shaped UWB monopole antenna is reported [4] with three notched band function. By etching out U-C shaped slot in the radiating patch dual-notched function is obtained while the third notch is obtained by a U-shaped slot in the feed line. A UWB antenna with octagonal shape radiating patch, by attaching three beveled L-shaped stubs of a quarter-wavelength to the ground plane of the slot near the feed line, an extra band at 2.4 GHz (Bluetooth band) and two notched bands centered at 3.5 GHz (WiMAX) and 5.8 GHz (WLAN) are created [5]. By using two folded slots and a T-shaped stub on a Coplanar-Waveguide (CPW) fed circular ring, a UWB antenna with triple-notched characteristics is achieved [6]. A UWB monopole antenna consisting of elliptically shaped radiating patch with fractal slots for triple band-notched function is designed [7]. Three notched bands with a broken ∩-shaped slot are reported in [8], and the notched band frequencies are centered at 2.40 GHz,

\* Corresponding author: Yogendra Kumar Awasthi (yogendra@mru.edu.in).
[1] Department of Electronics & Communication Engineering, Aravali College of Engineering & Management, Faridabad, India.
[2] Antenna Fabrication & Measurement Laboratory, Electronics & Communication Engineering, Manav Rachna University, Faridabad, India. [3] Department of Electronics, Sri Aurobindo College, University of Delhi, New Delhi, India.

3.80 GHz and 5.50 GHz, respectively. An enhanced bandwidth triple band-notched UWB antenna is reported in [9] which also contains a rectangular patch with two bevels, by inserting two round-shaped slots of half wavelength in the radiating patch and by etching out a pair of C-shaped slots in the ground plane. Fractal Koch and T-shaped stub for a triple-notch UWB monopole antenna is presented [10], centered at 2.00 GHz, 3.50 GHz and 5.50 GHz, respectively. Triple notched band resonators in a single design are fabricated [11] by inserting a C-shape slot at main radiator, complimentary SRR (CSRR) at ground plane and an inverted U-shape slot at the center of the patch, resulting in narrow band rejection of triple-notched band. Two bevels along with two round-shape slots in a rectangular patch and a pair of C-shaped slots in the ground plane re responsible for a triple-notched band UWB antenna [12]. A spiral slot on the rectangular CPW fed monopole antenna is presented [13], and by varying the length of the single spiral slot, triple notches with central frequencies of 3.57 GHz, 5.12 GHz and 8.21 GHz, respectively, are reported. A semicircular radiating patch with modified ground plane and two bevels at the upper edge results in a UWB monopole antenna. Furthermore, WiMAX and WLAN notched bands are obtained by etching two round-shaped slots and a rotated V-shaped slot on the ground plane, which results in X-band downlink satellite communication system [14]. A radiating patch with two bevels at the bottom edge and the modified ground plane with dual bevels of its upper edge result in a UWB monopole antenna. By placing a symmetrical pair of slots along patch length with CSRR on the patch and simultaneously introducing CSRR on the ground plane, triple notched characteristics are obtained [15]. A planar elliptical shape UWB antenna with multiple fractal-shaped slots and a Sierpinski fractal curved-shape ring resonator at the back of the substrate is reported for triple-notch distinctiveness [16, 17]. A small printed flower-shape dual-notched UWB-extended bandwidth antenna for wireless applications is obtained by inserting two C-shaped slots on the radiating patch [18]. A CPW-fed circular shape radiating patch on silicon with resistivity $\rho \geq 80\,\Omega$-m includes two rectangular slots for WiMAX and WLAN which are published [19]. An antenna is fabricated on silicon for ESPACENET sensor satellite application with operating frequency from 30.00 GHz–150.0 GHz with maximum gain of 5.50 dBi [20]. For imaging applications at 94 GHz, two high-gain Quasi-Yagi printed antennas are developed on silicon [21]. A millimeter-wave antenna on silicon is designed, which enables complex, low cost systems for high rate communications and sensing applications, and multiple components, such as impulse generator circuit, transmitter circuit and loop antenna, are also designed on silicon [22, 23]. An on-chip antenna on silicon using LC resonator is designed [24–26] which contains a stacked capacitor and a spiral inductor. A triple-notch UWB antenna with multiple wireless applications is fabricated [27] which covers measured bandwidth from 2.49 GHz–19.41 GHz.

In this paper, a CPW-fed circular monopole UWB antenna with dimension of $20 \times 20 \times 0.5\,\text{mm}^3$ is designed on silicon which provides a wide bandwidth (3.00 GHz–13.74 GHz) along with triple band-notch characteristics centered at ($f_{\text{Notch}}$) 3.47 GHz (VSWR = 43.29), 5.66 GHz (VSWR = 21.84) and 7.37 GHz (VSWR = 48.35), respectively.

## 2. ANTENNA DESIGN ANALYSIS

The proposed CPW-fed UWB monopole antenna is designed on silicon with thickness 0.7 mm and fed by 50 $\Omega$ microstrip line which is shown in Figure 1(a) with relative permittivity $\varepsilon_r = 11.9$, $\tan\delta = 0.012$. Radiating patch has a circular shape of radius $R$ which is calculated by the following Equations (1)–(2) [25]:

$$R = \frac{F}{\sqrt{\left(1 + \frac{2h_{si}}{\pi\varepsilon_r F}\left[\ln\left\{\frac{\pi F}{2h_{si}}\right\} + 1.7726\right]\right)}}; \quad \text{where } F = \frac{8.791 \times 10^9}{f_r \times \sqrt{\varepsilon_r}} \tag{1}$$

$h_{si}$ = height of silicon-substrate in mm, $\varepsilon_r$ = relative permittivity of the substrate, $f_r$ = resonating frequency in GHz and $\pi = 22/7$.

The effective radius, $R_e$, of the patch antenna is given by

$$R_e = R\sqrt{1 + \frac{2h_{si}}{\pi\varepsilon_r R}\left[\ln\left\{\frac{\pi R}{2h_{si}}\right\} + 1.7726\right]} \tag{2}$$
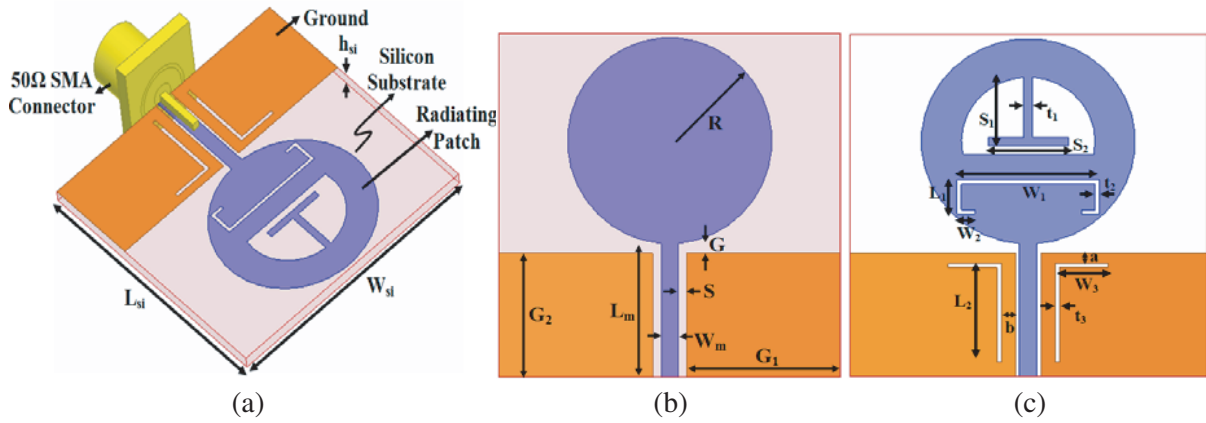
**Figure 1.** Geometry of proposed UWB antenna. (a) 3-D view, (b) front view without notched bands, (c) front view with notched bands.
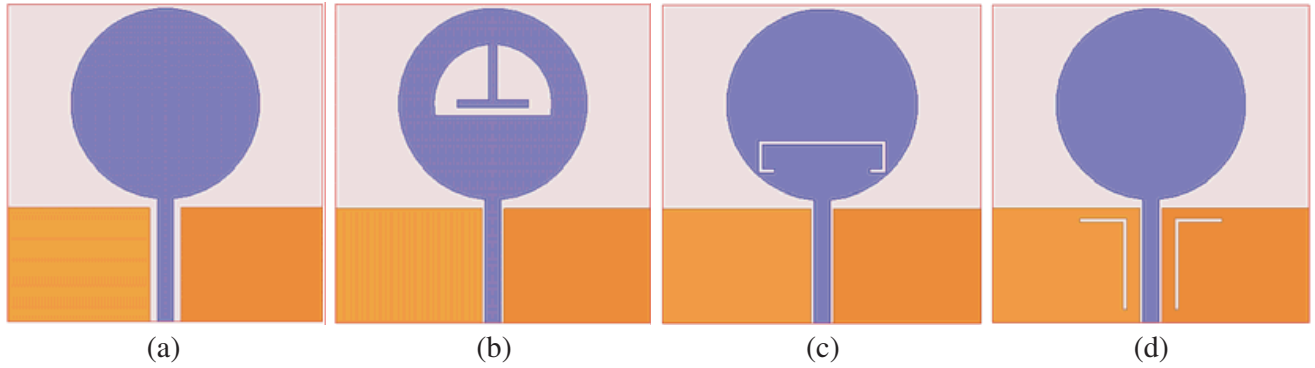


**Figure 2.** All steps of proposed UWB antenna. (a) CPW-fed, (b) WiMAX notch, (c) WLAN notch, (d) X-band downlink satellite communication system notch.

Figures 1(a)–(c) represent geometry of the proposed antenna. In Figure 1(c), the radiating patch consists of an inverted T-shape stub which eliminates first notched WiMAX band (3.30 GHz–3.80 GHz) and a C-shaped slot which removes WLAN band (5.150 GHz–5.825 GHz).

The third notch X-band downlink satellite communication system (7.25 GHz–7.75 GHz) is removed by etching a pair of rotated L-shaped slots in ground plane. The lengths of the first, second and third notches are calculated using Equations (3)–(4) respectively, and widths of notches are optimized arbitrarily and discussed in Section 3.2 [27].

$$L_{\text{Notch Band}} = c/\left(2 \times f_{\text{Notch}}\sqrt{\varepsilon_{reff}}\right) \tag{3}$$

$$\varepsilon_{reff} = \frac{\varepsilon_r + 1}{2} + \frac{\varepsilon_r - 1}{2}\left[1 + 12\frac{h_{si}}{W_m}\right]^{-\frac{1}{2}} \tag{4}$$

where $c$ is the speed of EM wave in free space and given by $c = 3 \times 10^8$ m/sec. From [17], effective relative permittivity of the substrate is calculated $\varepsilon_{reff}(w_m/h_{si}, \varepsilon_r, f)$. The optimal dimensions of the designed antenna are as follows: $R = 6.0$ mm, $G = 0.35$ mm, $S = 0.20$ mm, $W_m = 1.00$ mm, $L_m = 7.75$ mm, $G_1 = 9.30$ mm, $G_2 = 7.20$ mm, $S_1 = 3.5$ mm, $S_2 = 4.5$ mm, $W_1 = 8.0$ mm, $W_2 = 1.0$ mm, $L_1 = 2.0$ mm, $W_3 = 3.0$ mm, $L_2 = 6.0$ mm, $t_1 = 0.5$ mm, $t_2 = t_3 = 0.25$ mm, $W_{si} = 20.0$ mm, $L_{si} = 20.0$ mm, $h_{si} = 0.70$ mm, $W_3 = 9.0$ mm, $W_4 = 3.80$ mm.

Figure 2(a) shows configuration of the proposed antennas used for multi-resonance, and Figures 2(b)–(d) represent triple band-notch performance. Figure 3 shows the simulated VSWR results in respective of Figure 2. Antenna design starts with a circular radiating patch as shown in Figure 2(a)
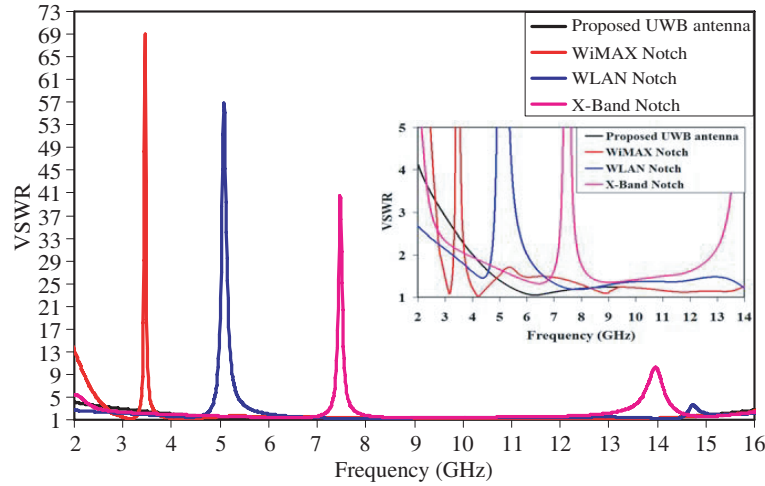
**Figure 3.** VSWR comparison from proposed UWB monopole to individual notch proposed antenna.

with optimized radius $R$, and *proposed UWB antenna* covers impedance bandwidth from 3.90 GHz–15.26 GHz. As observed from Figure 2(b), by inserting an inverted-T shaped stub on the radiating patch, intended interfere *WiMAX Notch* (3.31 GHz–3.76 GHz) is eliminated with high band rejection at 3.45 GHz with VSWR = 68.97.

WLAN band is notched by etching a C-shaped slot on the circular patch as shown in Figure 2(c) and corresponding VSWR represented in Figure 3 by *WLAN Notch* with notched bandwidth from 4.71 GHz–6.01 GHz, high band rejection centered at 5.04 GHz with VSWR = 56.93. The third notch intended for removal of X-band downlink satellite communication system is obtained by etching a pair of half-wavelength rotated L-shaped slots in the ground plane which is shown in Figure 2(d) and corresponding observation from Figure 3, notched bandwidth of 7.14 GHz–7.87 GHz with VSWR = 40.55 centered at 7.47 GHz.

## 3. PARAMETRIC STUDY OF OPTIMIZED UWB ANTENNA PARAMETERS AND NOTCHED BANDS

The proposed antenna is investigated and optimized by a full-wave FEM solver. Parametric study is carried out for the initial design of UWB antenna followed by the effect of individual notched bands. The centre frequency of notched bands along with peak value of VSWRs is controlled by the length of T-shaped stub, C-shaped slot on radiating patch and inverted L shaped-slots in ground plane, whereas bandwidth of notched bands are also controlled by the width of stub/slots, as discussed below.
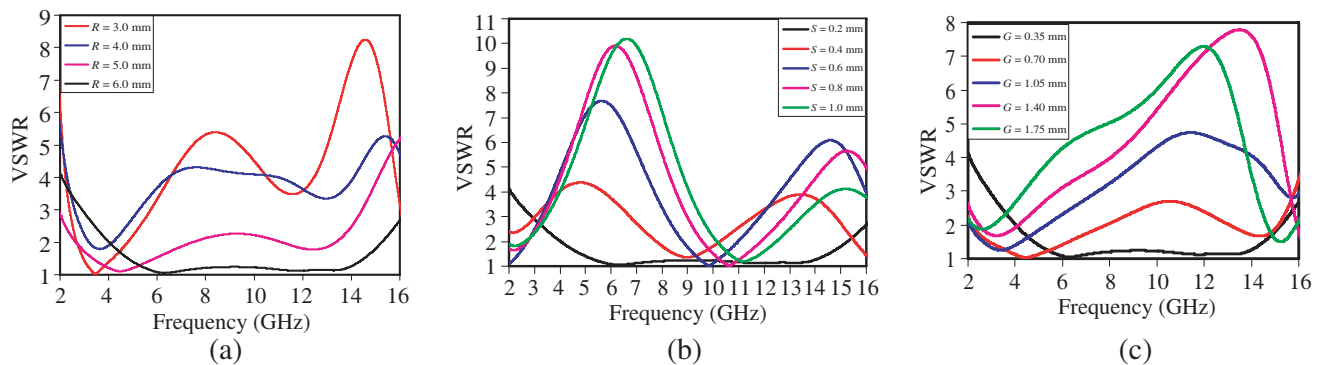


**Figure 4.** Parametric variation of (a) radius $R$, (b) $S$, (c) $G$.

### 3.1. Effect of Radiating Patch Radius ($R$), Effect of Slot Width ($S$) & Gap between Ground and Patch of Proposed UWB Antenna

Figure 4(a) shows variation of radius $R$ which corresponds to radiating patch. As radius $R$ is varied from 3.0 mm to 6.0 mm, VSWR curve improves indicating good impedance match. Optimized value for radiating patch ($R = 6.0$ mm) covers operating band from 3.94 GHz–15.26 GHz. Figures 4(b)–(c) represent variation of slot width ($S$) and the gap between ground and radiating patch ($G$). As $S$ is varied from 0.2 mm to 1.0 mm, impedance matching in the entire operating band worsens. Also, by varying gap between ground and radiating patch from 0.35 mm to 1.75 mm, improvement of impedance match deteriorates. Optimizing values of $S$ & $G$ are 0.2 mm and 0.35 mm respectively which covers impedance bandwidth of 3.94 GHz–15.26 GHz.

### 3.2. Effect of Stub Length $S_1$ and $S_2$ for WiMAX Notch

For the first notch (3.30 GHz–3.80 GHz), simulated parametric variation of $S_1$ with constant value of $S_2$ (4.50 mm) is shown in Figure 5(a). By varying length of $S_1$ of the T-shaped stub from 1.50 mm to 3.50 mm, wide shift of band-notch (shown by arrow) is observed from 3.69 GHz to 4.15 GHz with VSWR varying from 43.11 to 68.97, respectively. The length $S_1$ is tuned at 3.50 mm for the proposed antenna. Figure 5(b) represents simulated parametric variation of $S_2$ with constant value of $S_1$ (3.50 mm), and by varying length of $S_2$ from 2.50 mm to 4.50 mm of T-shaped stub, wide shift of (shown by arrow) band-notch is observed from 3.61 GHz–4.18 GHz to 3.31 GHz–3.71 GHz with VSWR varying from 48.90 to 68.86, respectively.

Length $S_2$ is tuned at 4.50 mm for the designed antenna. The total length of the T-shaped stub is given by $L_{\text{WiMAX}} = S_1 + S_2$.
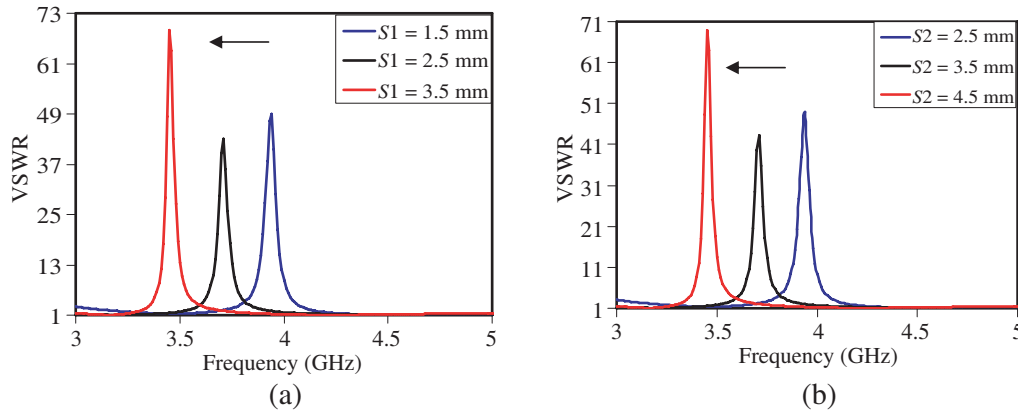


**Figure 5.** Simulated parametric variation of for WiMAX band (3.30 GHz–3.80 GHz). (a) $S_1$, (b) $S_2$.
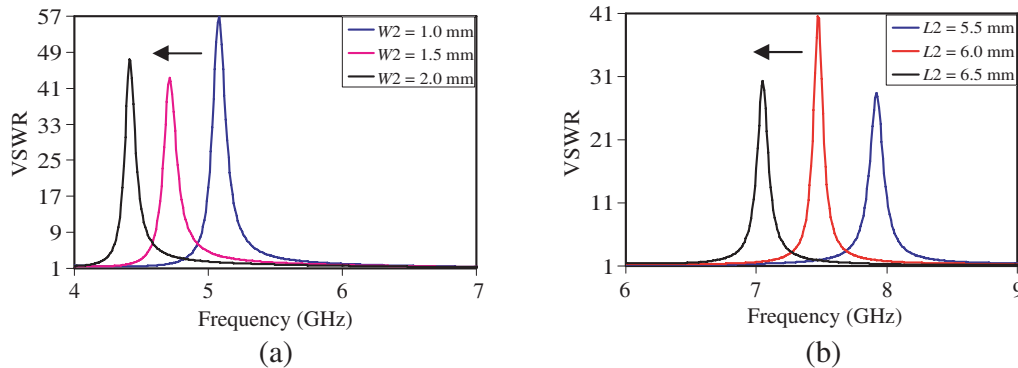


**Figure 6.** Simulated parametric variation of (a) $W_2$ for WLAN band notch, (b) $L_2$ for X-band downlink satellite communication system notch band.

### 3.3. Effect of Slot Length $W_2$ for WLAN Notch Band

For the second notch (5.150 GHz–5.825 GHz) as shown in Figure 6(a), $W_2$ is varied from 1.0 mm to 2.0 mm, and the corresponding change in VSWR at notches is 56.93–47.07 (shown by arrow).

Optimizing value of $W_2$ for the proposed antenna is 1.0 mm. Total length of the C-shaped slot is calculated as $L_{\text{WLAN}} = W_1 + 2(W_2 + L_1)$ mm.

### 3.4. Effect of Slot Length $L_2$ for X-Band Downlink Satellite Communication System Notch Band

For the third notch (7.25 GHz–7.75 GHz) as shown in Figure 6(b), $L_2$ is varied from 5.5 mm to 6.5 mm, and the corresponding change in VSWR at notches is 47.17–28.44 (shown by arrow). Optimizing value of $L_2$ for the proposed antenna is 6.0 mm. Total length of the inverted L-shaped slot is calculated as $L_{\text{X-Notch}} = W_3 + L_2$.

### 3.5. Effect of Stub Width $t_1$ and Slot Width $t_2/t_3$

Table 1 concludes that the intended bandwidth for WiMAX notched band decreases as $t_1$ increases, but for WLAN and X-band notched bandwidth increases when $t_2$ & $t_3$ increases. $t_1 = 0.5$ mm and $t_2 = t_3 = 0.25$ mm are the optimized values of width of the T-shaped stub, C-shaped and inverted L-shaped slots.

**Table 1.** Parametric variation of notched-bandwidth by varying width of stub and slots ($t_1$, $t_2$, & $t_3$ as shown in Figure 1(c)).

| WiMAX Notch | | WLAN Notch | | X-Band Notch | |
|---|---|---|---|---|---|
| $t_1$ (mm) | BW (GHz) | $t_2$ (mm) | BW (GHz) | $t_3$ (mm) | BW (GHz) |
| 0.25 | 0.66 | 0.25 | 0.618 | 0.25 | 0.725 |
| 0.50 | 0.55 | 0.50 | 0.683 | 0.50 | 0.814 |
| 0.75 | 0.49 | 0.75 | 0.936 | 0.75 | 1.189 |

## 4. ANALYSIS OF SURFACE CURRENT DENSITY DISTRIBUTION & TIME DOMAIN FOR PROPOSED ANTENNA

Furthermore, to understand the phenomenon behind triple-notch performance, the simulated current distribution on the radiating patch and ground plane at the notched frequencies 3.47 GHz, 5.66 GHz and 7.36 GHz respectively is carried out and shown in Figures 7(a)–(c). It is observed from Figure 7(a) that current density is more concentrated within the T-shaped stub while Figures 7(b)–(c) show that the current density is distributed on the inner and outer edges of the C-shaped and inverted L-shaped slots. Due to this there is change in impedance of antenna. In addition, the strong current distributions around stub and slots at the notched frequency lead to near-field radiation counteracted, due to which high energy is reflected back to the input port, and the band-notched characteristics are achieved.

It is also noticed that in Figures 7(a)–(c) there is very low mutual coupling at notched frequencies, which indicates that each rejected band can be controlled independently. In addition, it is also observed that at entire frequency passband except triple band-notches, the surface current is distributed uniformly over the antenna.

Figure 8(a) represents the pulse handling capability of the proposed notched-band antenna. The transmitter and receiver are spaced at a distance $d = 250$ mm for far-field results. Pulse from the transmitter is transmitted between two identical antennas (transmitter and receiver) oriented face-to-face and side-to-side. Pulse distortion which is one of the characteristics of UWB signals is essentially determined by their wide bandwidth of the proposed antenna. Better impedance matching over the proposed frequency band is observed to minimize reflection loss and avoid pulse distortion. The main reason of signal distortions is the mismatch between source pulse and the antenna.
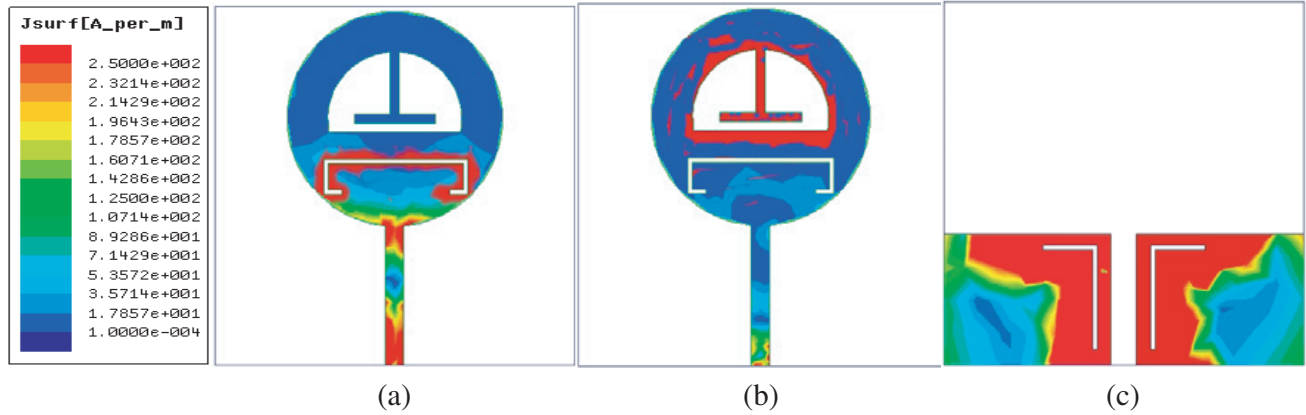
**Figure 7.** Simulated current density distribution. (a) 3.47 GHz, (b) 5.66 GHz, (c) 7.36 GHz.
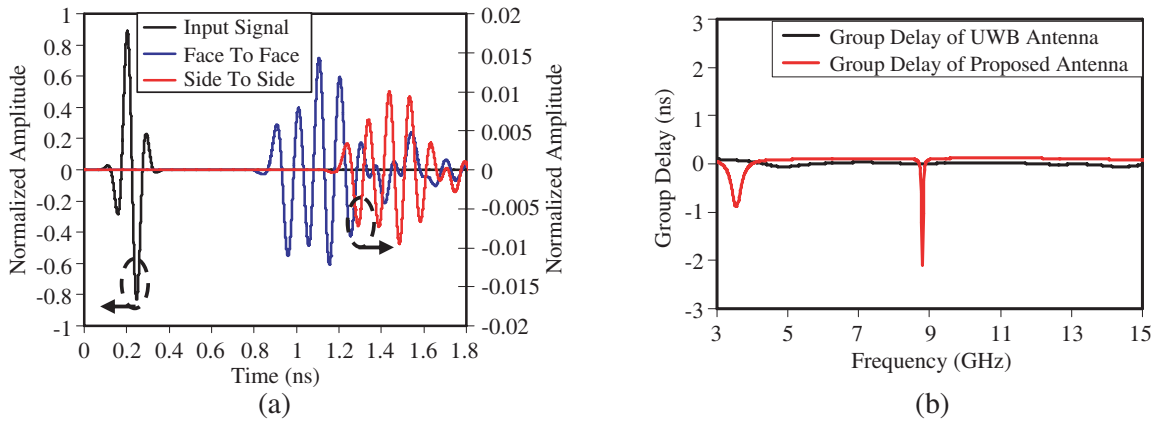


**Figure 8.** (a) Time domain analysis (input signal and impulse response), (b) group delay.

Therefore, some frequency components cannot be transmitted effectively by the antenna, leading to distortions of the received signal. From observation, more signals are received when antennas are placed in Face-to-Face orientation rather than Side-to-Side orientation. Figure 8(b) represents group delay of the proposed antenna without and with notched bands. Group delay is an important parameter for UWB and other communications since it can judge the distortion of transmitted pulses. For a perfect pulse transmission, the group delay should be close to a constant within the entire band. It can also be concluded that the proposed antenna has perfect performance in this aspect, which makes it quite suitable for UWB as well as other higher band wireless communication.

## 5. EQUIVALENT CIRCUIT ANALYSIS

In order to analyze the theory behind UWB and triple-notched band characteristics, equivalent circuit model based on input impedance response is carried out which is obtained from a full-wave EM solver. Based on input impedance characteristics, UWB antenna can be modeled as the result of several adjacent resonance circuits which equally represents parallel RLC circuit [26], and equivalent circuit model based on the concept for UWB-Extended bandwidth antenna is shown in Figure 9(a).

$$Z_{La} = \sum_{j=1}^{n} \frac{j\omega R_j L_j}{R_j \left(1 - \omega^2 L_j C_j\right) + j\omega L_j} \tag{5}$$

Either from simulated or measured results corresponding to resonances ($Z_{La}$), values of consecutive parameters of the equivalent circuit model are calculated ($R_j$, $L_j$, $C_j$) by Equation (5). Figure 10(a)

represents input impedance of antenna shown in Figure 1(b). Real and imaginary parts of input impedance value vary around $50\,\Omega$ and zero ohms, respectively. In the case of notched-band characteristics (WiMAX, WLAN & X-Band downlink satellite system), high mismatch impedance is required which is shown in Figure 10(b) and Figure 10(c).

In the case of WiMAX notched-band characteristics, at $3.30\,\mathrm{GHz}$, real part of impedance is $21\,\Omega$ whereas imaginary part of impedance shifts from negative to positive value which corresponds to series resonance circuit. Furthermore, at $3.60\,\mathrm{GHz}$, real part of impedance is $284.39\,\Omega$, and correspondingly imaginary impedance shifts from positive to negative value which leads to parallel resonance circuit. This
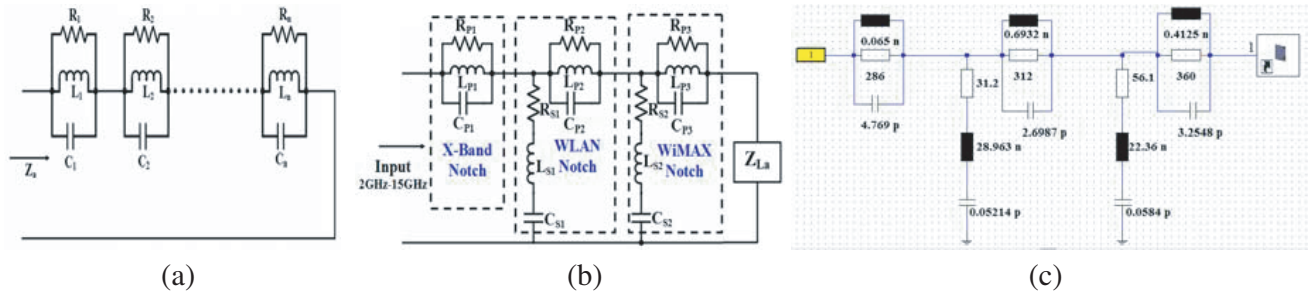


**Figure 9.** Equivalent circuit model for proposed antenna. (a) UWB, (b) triple notched, (c) snapshot of proposed antenna in CST design studio.
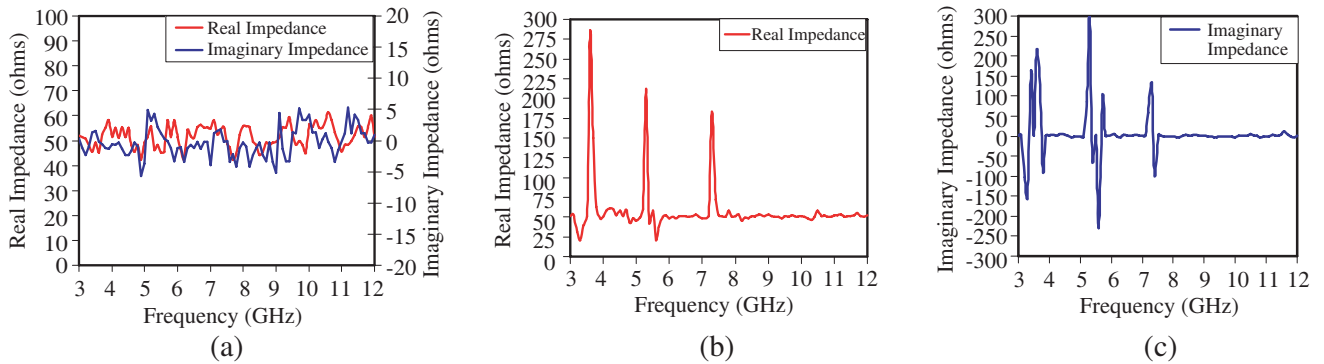


**Figure 10.** Simulated input impedance of proposed antenna. (a) UWB, (b) real impedance of triple notched band, (c) imaginary impedance of triple notched band.
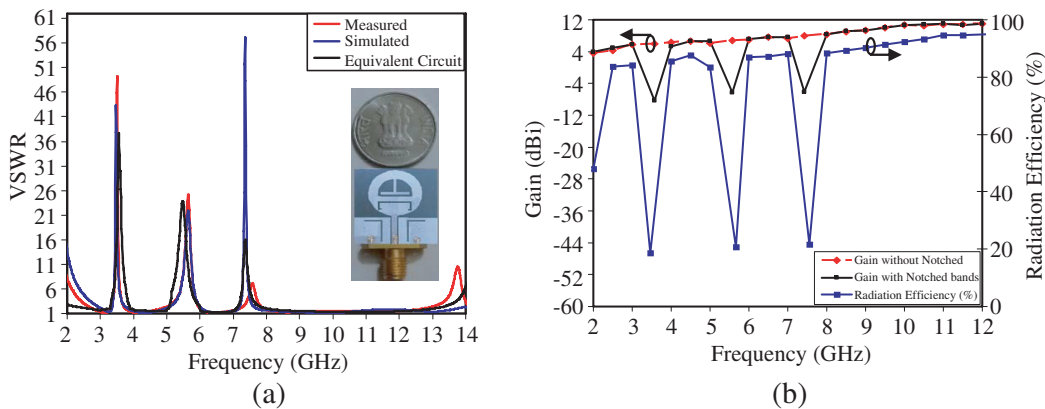


**Figure 11.** Proposed antenna. (a) Measured and simulated VSWR, (b) measured gain (dBi) and radiation efficiency.

combination of Series-Parallel resonance circuits are represented in Figure 9(b), and the corresponding results are shown in Figures 10(b)–(c). In the case of WLAN band, real impedance value is $212\,\Omega$ at $5.30\,\text{GHz}$, and the corresponding imaginary impedance value shifts from positive to negative value. Also, for frequency $5.60\,\text{GHz}$, real part of impedance value corresponds to $21\,\Omega$, and imaginary value changes from negative to positive value. Combining both the analysis for WLAN notch ($5.30\,\text{GHz}$ and $5.60\,\text{GHz}$), equivalent resonant circuit is the combination of Parallel and Series RLC resonance circuit. For an X-band downlink satellite system ($7.25\,\text{GHz}$–$7.75\,\text{GHz}$), at frequency $7.60\,\text{GHz}$, real part of input impedance is $183.36\,\Omega$, and imaginary value changes from positive to negative. This leads to a parallel RLC resonance circuit. For remaining UWB-extended bandwidth, real part of impedance varies around $50\,\Omega$, and imaginary part varies around zero ohms. Also, VSWR curve is plotted for the entire triple-notched UWB antenna which is compared by simulated and measured results represented in Figure 11(a). At notched frequencies, either open or short (high or low input impedance) at the antenna input terminals results in mismatch from $50\,\Omega$ impedance, and large reflections at input and band-notch characteristics are observed. Resonant frequencies and corresponding bandwidth of the series and parallel resonance circuits for Figures 9(b)–(c) are calculated by following equations

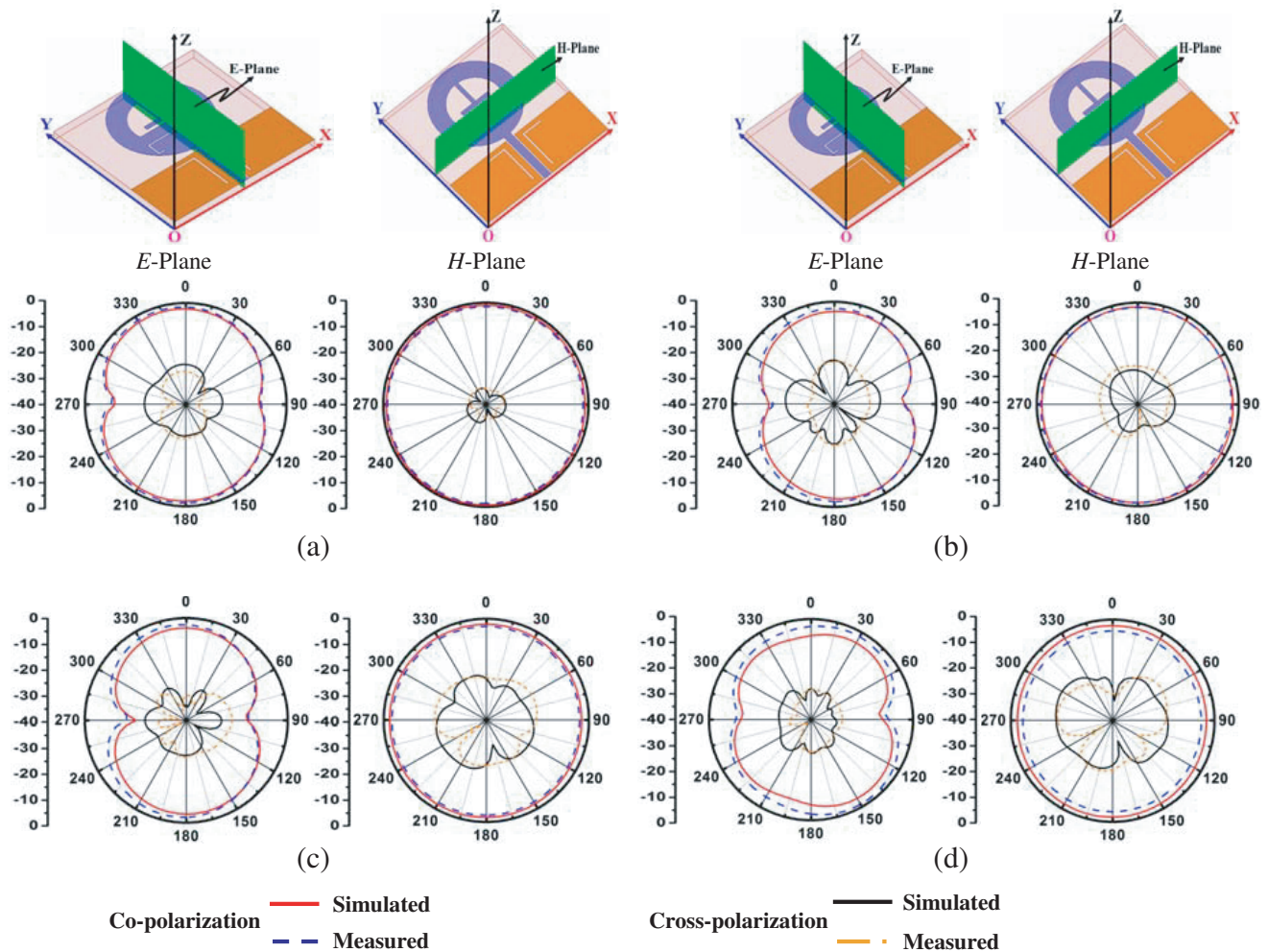$$\omega_{SR} = \frac{1}{\sqrt{L_{sn} \times C_{sn}}} \tag{6}$$



**Figure 12.** Measured radiation pattern of $H$ and $E$-plane in dB at (a) $4.5\,\text{GHz}$, (b) $7.0\,\text{GHz}$, (c) $9.0\,\text{GHz}$, (d) $11.0\,\text{GHz}$.

$$\mathrm{BW}_{SR} = \frac{R_{sn}}{L_{sn}} \tag{7}$$

$$\omega_{PR} = \frac{1}{\sqrt{L_{pn} \times C_{pn}}} \tag{8}$$

$$\mathrm{BW}_{PR} = \frac{1}{R_{pn} \times C_{pn}} \tag{9}$$

$\omega_{SR}$, $\omega_{PR}$ are the series & parallel resonant frequencies, and $\mathrm{BW}_{SR}$, $\mathrm{BW}_{PR}$ are the corresponding bandwidths which are noted from Figures 10(b)–(c) along with the values of $R_{sn}$ & $R_{pn}$. Using the noted values, the values of $L_{sn}$, $C_{sn}$, $L_{pn}$ and $C_{pn}$ for the equivalent circuit in Figure 9(b) are calculated by Equations (6)–(9) where $n = 1, 2, 3, \ldots$. Figure 9(c) represents a snapshot of CST Design studio where equivalent circuit model is constructed using RLC components for proposed triple-notched band antenna. Optimized circuit component (RLC) values are tabulated in Table 2.

## 6. EXPERIMENTAL RESULTS

Figure 11(a) validates the proposed UWB antenna with triple-notched band characteristics. There is a slight disagreement between simulated and measured results due to reasons such as impedance match between SMA connector and Microstrip soldered point. Measured rejection peak VSWRs 49.24, 25.22 & 6.75 correspond to 3.50 GHz, 5.56 GHz and 7.61 GHz respectively with measured bandwidth of the proposed antenna 3.00 GHz–13.74 GHz.

Measured gain of the proposed antenna and radiation efficiency are shown in Figure 11(b). A negative peak gain is noted in notched band: 8.36 dBi at 3.57 GHz, 6.38 dBi at 5.58 GHz and 6.10 dBi at 7.42 GHz, which confirms that antenna does not radiate in these three notched bands whereas gain

**Table 2.** Optimized RLC components for notched bands.

| Resistance (R) | Value ($\Omega$) | Capacitance (C) | Value (pF) | Inductance (L) | Value (nH) |
|:---:|:---:|:---:|:---:|:---:|:---:|
| $R_{s1}$ | 31.2 | $C_{s1}$ | 28.963 | $L_{s1}$ | 0.05214 |
| $R_{s2}$ | 56.1 | $C_{s2}$ | 22.36 | $L_{s2}$ | 0.058 |
| $R_{p1}$ | 286 | $C_{p1}$ | 0.065 | $L_{p1}$ | 4.769 |
| $R_{p2}$ | 312 | $C_{p2}$ | 0.6932 | $L_{p2}$ | 2.6987 |
| $R_{p3}$ | 360 | $C_{p3}$ | 0.4125 | $L_{p3}$ | 3.2548 |

**Table 3.** Comparison of the proposed antenna parameters (measured) with several existing designs.

| Freq. (GHz) | VSWR First Notch | Peak Gain (dBi) | Freq. (GHz) | VSWR Second Notch | Peak Gain (dBi) | Freq. (GHz) | VSWR Third Notch | Peak Gain (dBi) | Dimensions of Antenna (mm²) |
|:---:|:---:|:---:|:---:|:---:|:---:|:---:|:---:|:---:|:---:|
| 3.5 | 6.04 | −2.00 | 5.6 | 5.63 | −1.98 | 7.5 | 4.38 | −3.00 | 30 × 35 [2] |
| 2.4 | 4.68 | −5.00 | 3.8 | 4.71 | −3.98 | 6.0 | 5.04 | −3.42 | 30 × 35 [3] |
| 3.4 | 4.50 | 0.12 | 5.5 | 4.68 | 0.00 | 7.7 | 5.14 | −1.53 | 30 × 30 [4] |
| 2.4 | 7.98 | −8.20 | 4.3 | 7.65 | −11.4 | 5.9 | 6.33 | −6.33 | 23 × 28 [5] |
| 3.3 | 14.3 | −0.81 | 5.5 | 14.1 | 0.22 | 10.6 | 10.4 | −5.36 | 41 × 45 [7] |
| 3.3 | 6.85 | −4.96 | 5.6 | 6.12 | −4.11 | 7.7 | 5.18 | −3.98 | 22 × 31 [9] |
| 3.5 | 7.32 | −6.38 | 5.8 | 6.91 | −6.71 | 7.7 | 6.12 | −4.12 | 20 × 31 [12] |
| 3.3 | 7.13 | −6.11 | 5.6 | 6.93 | −2.58 | 7.6 | 6.12 | −4.03 | 25 × 27 [14] |
| 5.6 | 21.2 | −2.18 | 7.1 | 20.1 | −4.93 | 8.1 | 16.1 | −2.98 | 41 × 51 [16] |
| **3.6** | **16.2** | **−6.62** | **5.6** | **22.4** | **−8.75** | **7.6** | **6.38** | **−5.32** | **20 × 20 ∗ P** |

∗P Proposed antenna

(5.08–11.05 dBi) is almost matched without notched band antenna. The proposed antenna also exhibits good radiation efficiency (84–95%) across the entire bandwidth except in three notched bands as 18.65%, 20.66% and 21.69% at 3.46 GHz, 5.66 GHz and 7.55 GHz, respectively.

Figure 12 depicts the measured normalized radiating patterns of proposed antenna including co- & cross-polarizations in the $H$-plane ($x$-$z$ plane) and $E$-plane ($y$-$z$ plane). Nearly omnidirectional radiation characteristics are observed with less co-polarization in $H$-plane and small electric dipole in $E$-plane. At higher frequencies, it is also observed that cross polarization increases to some extent because of increase in area of radiation.

Comparison of the proposed antenna with published works at various parameters as maximum VSWR at center notched frequency with gain and size is shown in Table 3. As observed, peak gain rejections at notched frequencies 3.60 GHz, 5.60 GHz & 7.60 GHz are $-6.62$ dBi, $-8.75$ dBi & $-5.32$ dBi, respectively. Also, with compact design, the proposed antenna covers bandwidth of 10.74 GHz which includes UWB & X-band applications.

# 7. CONCLUSIONS

A compact triple band-notched $20 \times 20\,\text{mm}^2$ Ultra-Wideband antenna was fabricated on silicon and tested, which is also capable for usage in wireless services including close range radar (8–12 GHz) in X-band. In this paper, the antenna exhibits radiation efficiency and gain, i.e., 84–95% and 5.08–11.05 dBi, respectively, is nearly omnidirectional in $H$-plane with dipole-like radiation characteristics in the $E$-plane throughout bandwidth. In a nutshell, the proposed antenna has shown salient properties which are applicable in multiple wireless transceivers for both indoor and outdoor usages including communications and sensors, low/high data rate, home network applications and RADAR.

# ACKNOWLEDGMENT

# REFERENCES

1. First Report and Order, "Revision of Part 15 of the Commission's rules regarding ultra wideband transmission systems," Federal Communications Commission (FCC), FCC 02-48, 2002.

2. Srivastava, G., S. Dwari, and B. K. Kanaujia, "A compact triple band notch circular ring antenna for UWB applications," *Microwave and Optical Technology Letters, IEEE Antennas and Wireless Propagation Letters*, Vol. 57, No. 3, 668–672, 2015.

3. Zhang, Y., W. Hong, C. Yu, Z. Q. Kuai, Y. D. Don, and J. Y. Zhou, "Planar ultra wideband antennas with multiple notched bands based on etched slots on the patch and/or split ring resonators on the feed line," *IEEE Transactions on Antennas & Propagation*, Vol. 56, No. 9, 3063–3068, September 2008.

4. Tomar, S. and A. Kumar, "Design of a triple band-notched UWB planar monopole antenna," *Journal of Microwaves, Optoelectronics and Electromagnetic Applications*, Vol. 14, No. 2, 1–13, 2015.

5. Taheri, M. M. S., H. R. Hassani, and S. M. A. Nezhad, "UWB printed slot antenna with Bluetooth and dual notch bands," *IEEE Antennas and Wireless Propagation Letters*, Vol. 10, 255–258, 2011.

6. Li, Y., S. Chang, M. Li, and X. Yang, "A compact ring UWB antenna with tri-notch band characteristics using slots and tuning stub," *IEEE Conference*, 12–15, 2011.

7. Maiti, S., N. Pani, and A. Mukherjee, "Modal analysis and design a planar elliptical shaped UWB antenna with triple band notch characteristics," *IEEE Conference*, 13–15, 2015.

8. Lotfi, P., S. Soltani, and M. Azarmanesh, "Triple band-notched UWB CPW and microstrip line fed monopole antenna using broken ∩-shaped slot," *International Journal of Electronics and Communications*, Vol. 65, 734–741, 2011.

9.  Bakariya, P. S., S. Dwari, and M. Sarkar, "Triple band notch UWB printed monopole antenna with enhanced bandwidth," *International Journal of Electronics and Communications*, Vol. 69, 26–30, 2015.

10. Zarrabi, F. B., Z. Mansouri, N. P. Gandji, and H. Kuhestani, "Triple-notch UWB monopole antenna with fractal Koch and T-shaped stub," *International Journal of Electronics and Communications*, Vol. 70, 64–69, 2016.

11. Haroon, S., K. S. Alimgeer, N. Khalid, B. T. Malik, M. F. Shafique, and S. A. Khan, "A low profile UWB antenna with triple band suppression characteristics," *Wireless Personal Communication*, Vol. 82, 495–507, 2015.

12. Bakariya, P. S., S. Dwari, and M. Sarkar, "A triple band notch compact UWB printed monopole antenna," *Wireless Personal Communication*, Vol. 82, 1095–1106, 2015.

13. Das, S., D. Mitra, and S. R. B. Chaudhuri, "Design of UWB planar monopole antennas with etched spiral slot on the patch for multiple band-notched characteristics," *International Journal of Microwave Science and Technology*, 1–10, 2015.

14. Venkata, S. K., M. Rana, P. S. Bakariya, S. Dwari, and M. Sarkar, "Planar ultrawideband monopole antenna with tri-notch band characteristics," *Progress In Electromagnetics Research C*, Vol. 46, 163–170, 2014.

15. Sarkar, M. S. Dwari, and A. Daniel, "Printed monopole antenna for ultra-wideband application with tunable triple band-notched characteristics," *Wireless Personal Communication*, Vol. 84, 2943–2954, 2015.

16. Gorai, A., A. Karmakar, M. Pal, and R. Ghatak, "Multiple fractal-shaped slots-based UWB antenna with triple-band notch functionality," *Journal of Electromagnetic Waves and Applications*, Vol. 27, No. 18, 2407–2415, 2013.

17. Verma, A. K., Y. K. Awasthi, and H. Singh, "Equivalent isotrophic relative permittivity of microstrip on multilayer anisotrophic substrate," *International Journal of Electronics*, Vol. 96, No. 8, 865–875, August 2009.

18. Sharma, M., Y. K. Awasthi, H. Singh, R. Kumar, and S. Kumari, "Design of compact Flower shape dual notched-band monopole antenna for extended UWB wireless applications," Frequenz, DOI 10.1515/freq-2016-0065, 2016.

19. Karmakar, A. and K. Singh, "Planar monopole ultra wideband antenna on silicon with notched characteristics," *International conference on Microelectronics, Circuits and Systems*, 17–20, 2014.

20. Haridas, N., R. Zhang, A. E. Rayis, A. Erdogan, T. Arslan, A. Bunting, and A. J. Walton, "Multiband micro antenna on Silicon substrate," *IEEE Conference*, 1–8, 2009.

21. Haraz, O. M., M. A. Rahman, N. A. Khalli, S. Alshebeili, and A. R. Sebak, "Performance investigations of quasi-Yagi loop and dipole antennas on silicon substrate for 94 GHz applications," *International Journal of Antennas and Propagation*, 1–9, 2014.

22. Moussa, H. B. E., F. Torres, G. Z. E. Nashef, B. Barelaud, and E. Ngoya, "Integrated on-chip antenna on silicon-substrate for millimeter-wave applications," *IEEE Conference*, September 2013.

23. Ozdemirli, A., M. M. Bilgic, B. Tar, K. Yegin, and U. Cilingiroglu, "On-chip antenna design for UWB applications," *IEEE Conference*, July 2015.

24. Okabe, K., W. Lee, Y. Harada, and M. Ishida, "Silicon based on-chip antenna using LC resonator for near-field RF systems," *Solid-State Electronics*, Vol. 67, 100–104, 2012.

25. Chowdhury, B. B., R. De, and M. Bhowmik, "A novel design for circular patch fractal antenna for multi band applications," *IEEE International Conference Signal Processing and Integrated Networks*, 449–453, 2016.

26. Pandey, G. K., H. S. Singh, P. K. Bharti, and M. K. Meshram, "Design and analysis of multiband notched Pitcher-shaped UWB antenna," *International Journal of RF and Microwave Computer-Aided Engineering*, 795–805, 2016.

27. Sharma, M., Y. K. Awasthi, H. Singh, R. Kumar, and S. Kumari, "Compact printed high rejection triple band-notch UWB antenna with multiple wireless applications," *Engineering Science & Technology*, Vol. 19, 1626–1634, 2016.